BJP British Journal of Pharmacology

DOI:10.1111/bph.12323
www.brjpharmacol.org

RESEARCH PAPER

3,3′-Diindolylmethane ameliorates experimental hepatic fibrosis via inhibiting miR-21 expression

Zhengping Zhang[1], Zhongfei Gao[1], Wei Hu[1], Shan Yin[1], Chunming Wang[2], Yuhui Zang[1], Jiangning Chen[1], Junfeng Zhang[1,3] and Lei Dong[1,2]

[1]*State Key Laboratory of Pharmaceutical Biotechnology, School of Life Sciences, Nanjing University, Nanjing, China,* [2]*State Key Laboratory of Quality Research in Chinese Medicine, Institute of Chinese Medical Sciences, University of Macau, Macau, China, and* [3]*Jiangsu Engineering Research Center for microRNA Biology and Biotechnology, Nanjing, China*

Correspondence
Lei Dong and Junfeng Zhang, School of Life Science, Nanjing University, 1705 Mengminwei Building, 22# Hankou Rd., Nanjing, Jiangsu 210039, China.
E-mail: leidong@nju.edu.cn; jfzhang@nju.edu.cn

Keywords
Liver fibrosis; 3,3′-Diindolylmethane; hepatic stellate cells; miR-21; AP-1; Smad; TGF-β

Received
29 April 2013
Revised
26 June 2013
Accepted
21 July 2013

BACKGROUND AND PURPOSE

Hepatic fibrosis is a type of liver disease characterized by excessive collagen deposition produced by activated hepatic stellate cells (HSCs), and no appropriate drug treatment is available clinically. The microRNA, miR-21 exhibits an important role in the pathogenesis and progression of hepatic fibrosis. 3,3′-Diindolylmethane (DIM) is a natural autolytic product in plants and can down-regulate miR-21 expression. Here we have assessed the therapeutic effects of DIM against hepatic fibrosis and investigated the underlying mechanisms.

EXPERIMENTAL APPROACH

The effects of DIM on HSC activation were measured by analysing the expression of α-smooth muscle actin and collagen I in both HSC-T6 cell line and primary HSCs. Expression of miR-21 was also measured after DIM treatment and the therapeutic effect of DIM was further studied *in vivo*, using the model of hepatic fibrosis induced by thioacetamide in mice. The antagonist oligonucleotide, antagomir-21, was also used to suppress the effects of miR-21.

KEY RESULTS

DIM suppressed the central TGF-β signalling pathway underlying HSC activation by down-regulating the expression of miR-21. The decreased miR-21 expression was achieved by inhibiting the activity of the transcription factor, AP-1. Moreover, DIM blunted the activation phenotype of primary HSCs. Administration of DIM *in vivo* attenuated liver fibrosis induced by thioacetamide, as assessed by collagen deposition and profiles of profibrogenic markers.

CONCLUSIONS AND IMPLICATIONS

DIM shows potential as a therapeutic agent for the treatment of hepatic fibrosis.

Abbreviations

α-SMA, α-smooth muscle actin; ALT, alanine aminotransferase; AP-1, activation protein 1; AST, aspartate aminotransferase; COL1A1, collagen 1a1; HCC, hepatocellular carcinoma; HSCs, hepatic stellate cells; miRNAs, microRNAs; TAA, thioacetamide

Introduction

Liver fibrosis is a wound-healing process in response to chronic liver injuries, such as alcohol abuse, drug toxicity, viral infection and fatty liver disease associated with obesity, marked by progressive abnormal deposition of extracellular matrix (ECM). As hepatic fibrosis progresses, liver parenchyma and vascular architecture may be distorted and liver

function impaired, leading to liver failure and hepatocellular carcinoma (HCC), which are the major causes of morbidity and mortality worldwide (Hernandez-Gea and Friedman, 2011).

Activated hepatic stellate cells (HSCs) are identified as the main producers of ECM in liver and their activation represents the critical event in liver fibrogenesis. After liver injury, the quiescent HSCs trans-differentiate into myofibroblast-like cells that are characterized by the expression of α-smooth muscle actin (α-SMA). The canonical TGF-β/Smad2/3 signalling cascade mediates the activation of HSCs. TGF-β signals via its cognate receptors (TβRII and TβRI) to Smad2/3 proteins; phosphorylated Smad2/3 binds Smad4 and translocates into nucleus, enhancing the transcription of profibrogenic genes. As a regulatory system, Smad6/7 inhibits phosphorylation of Smad2/3 and/or could combine with Smurf proteins to degrade TβRII receptors, thus antagonizing the profibrogenic activities of TGF-β (Friedman, 2008). Although suppression of the TGF-β/Smad cascade has emerged as the primary strategy against fibrosis for patients with chronic liver diseases, more substantial innovations are required to make up for the current lack of clinically available drugs.

microRNAs (miRNAs) are a class of non-coding small RNAs, 18–22 nt in length, which bind to the target genes and thereby repress translation of target genes and/or induce degradation of target gene mRNA. miRNA-21 is one of the most important microRNAs up-regulated during fibrogenesis in different tissues (Thum *et al.*, 2008; Liu *et al.*, 2010; Zhong *et al.*, 2011). Furthermore, enhanced expression of miR-21 has been reported in the liver and correlated with the stage of fibrosis (Marquez *et al.*, 2010). Further, antagonizing the expression of miR-21 has achieved encouraging therapeutic effects against tissue fibrosis (Liu *et al.*, 2010; Chung *et al.*, 2013). Altogether, these studies suggest a significant role for miR-21 in fibrotic disease in different organs.

3,3′-Diindolylmethane (DIM) is a natural product formed during the autolytic breakdown of glucobrassicin present in food plants of the *Brassica* genus. DIM is a promising anti-tumour agent that has been widely studied in laboratory and clinical trials (McGuire *et al.*, 2006; Okino *et al.*, 2009; Rahman *et al.*, 2009). Furthermore, indole-3-carbinol, which could be easily metabolized to DIM and whose biological effects is mainly attributed to DIM, has been reported to significantly reduce miR-21 expression in lung cancer (Melkamu *et al.*, 2010).

Based on these observations, this study was designed to evaluate whether treatment with DIM would protect against thioacetamide (TAA)-induced experimental hepatic fibrosis. Furthermore, we investigated the possible mechanism(s) involved in the anti-fibrotic activity of DIM. Our present study indicated that DIM could suppress HSC activation via down-regulating miR-21 levels in HSCs by inhibiting activity of the transcription factor AP-1. Smad7, a direct target of miR-21, was up-regulated in both HSC-T6 cell lines and primary HSCs after DIM treatment. Up-regulated Smad7 expression antagonized the central TGF-β/Smad2/3 signalling pathway during HSC activation. Further studies in an animal models confirmed the therapeutic effects of DIM *in vivo*. Our present study suggests that DIM may be developed as a potential agent for the treatment of liver fibrosis.

Methods

Cells and animal model

The HSC-T6 is one of the most widely used cell line in studying hepatic fibrosis (Vogel *et al.*, 2000). For *in vivo* therapeutic study, the liver fibrosis model in mice is more stable and widely used. There are many studies using the rat HSC-T6 cell line and rat primary HSCs *in vitro*, while the *in vivo* studies were conducted in mice (Saxena *et al.*, 2002; Zhang *et al.*, 2009; Beaven *et al.*, 2011; Liu *et al.*, 2011). These studies demonstrated a good consistency between rat HSCs and mouse HSCs in cellular properties during liver fibrogenesis. Moreover, as for primary HSCs, to obtain rat primary HSCs is technically easier than to obtain mouse HSCs because the size of a rat liver is much bigger than that of a mouse, which is also specifically important for the experiments that need large amounts of cells from the same animal when testing drug activity. Thus, the *in vitro* study was conducted on HSC-T6 cells and rat primary HSCs, and the *in vivo* study was a hepatic fibrosis model in mice.

Establishment of experimental hepatic fibrosis and treatments

All animal care and experimental procedures complied with the use and care guidelines for the experimental animals from Jiangsu Province, China. All studies involving animals are reported in accordance with the ARRIVE guidelines for reporting experiments involving animals (Kilkenny *et al.*, 2010; McGrath *et al.*, 2010). A total of 40 animals were used in the experiments described here. Male ICR mice, (20 ± 2 g) of the same strain, were obtained from the Animal Centre of Yangzhou University (Yangzhou, China). Mice were randomly divided (each group contained at least 6 mice) and had free access to water and laboratory chow. Mice received i.p. injections of thioacetamide (TAA; 200 mg·kg^{-1}) twice weekly for 8 weeks, whereas control group received saline i.p. For the DIM treatment groups, 24 h after every TAA injection, a single dose of 100 μL DIM (concentrations of 2, 10 and 50 mg·mL^{-1}) or vehicle was administered i.p. Mice were killed at the indicated time points.

Isolation of primary HSCs

Primary HSCs were isolated according to the published protocols of Weiskirchen and Gressner (2005). The 8–12 month old male Sprague-Dawley rats (Yangzhuo University, Jiangsu Province, China) were anaesthetized with an i.p. injection of 15 mg·kg^{-1} pentobarbital. The liver perfusion buffer and liver digestion media were pre-warmed to 37°C and the perfusing buffer flow was maintained at 37° C. The liver was perfused *in situ* via the portal vein with heparin sodium buffer, while the inferior vena cava was used as outflow until the liver became pale. The perfusion was continued with collagenase H (3 mg·mL$^{-1;}$ Roche, Mannheim, Germany) and pronase (3 mg·mL^{-1}; Roche) buffer. Then, the liver was carefully removed and dissociated in digestion media II (0.5 mg·mL^{-1} collagenase and pronase, 0.2 mg·mL^{-1} DNase I) for further digestion. Afterwards, the liver cell suspension was filtered through gauze (100 μm) and centrifuged for 5 min at 50× *g*, 4°C to obtain parenchymal cells. The non-parenchymal cells were collected from the 50 g supernatant and washed twice

before density gradient centrifugation. A discontinuous density gradient (15 and 10%) was made by using OptiPrep™ (Oslo, Norway) according to manufacturer's instructions, and centrifuge at 1400× *g*, 4°C for 15 min while allowing the rotor to decelerate without braking. HSCs at the interface of mounting solution and low density barrier were collected. The purity was determined and generally exceeded 90%. The viability of the isolated cells was determined by Trypan blue staining and generally exceeded 95%.

Cell survival assay

Approximately 10 000 cells were plated into each well of 96-well flat-bottomed microtitre plates. Twelve hours later, the medium containing DIM (ranging from 2 to 20 $mg \cdot mL^{-1}$) was added to the cells. After 24 hours of incubation, 10 µL of the Cell Counting Kit-8 solution (Dojindo, Tokyo, Japan) was introduced into each well and incubated for 2 h. The plates were spectrophotometrically analysed with a microplate reader at 450 nm.

Cell treatments

HSC lines (rat HSC-T6 cells) or isolated primary rat HSCs were cultured in DMEM containing 10% FBS (Invitrogen, Camarillo, CA, USA) at 37°C with 5% CO_2 in a humid atmosphere.

HSC-T6 cells were cultured to 80–90% confluence and starved for 12 h; cells were then cultured with DIM or vehicle for further 12 h. Then, HSC-T6 cells were stimulated with TGF-β1, as indicated. DIM, in three different concentrations, was tested, and the 10 $\mu g \cdot mL^{-1}$ concentration was chosen. The concentration of 20 $\mu g \cdot mL^{-1}$ affected cell viability, whereas 5 $\mu g \cdot mL^{-1}$ had no obvious effect on the activation of HSC-T6 cells. When transfected with antagomirs, HSC-T6 cells were cultured to 70% confluence; 50 nM antagomir-21 or antago-ctrl was transfected into HSC-T6 cells.

For primary HSCs, cells were plated on plastic where primary cells underwent self-activation processes that mimicked the *in vivo* situation. 10 $\mu g \cdot mL^{-1}$ DIM or vehicle was added into the culture every other day; and as for the antagomir transfection groups, triple antagomir-21/antago-ctrl transfections (50 nM each) were conducted during the plastic culture. Further, the primary HSCs were harvested after 15 days of culture.

Cell transfection

The antagomir-21 or antago-ctrl was transfected with lipofectamine2000 (Invitrogen) following manufacturer's instructions. Generally, cells were plated and transfected at 70–80% confluence. The antagomirs were gently mixed with lipofectamine2000 in Opti-MEM Reduced Serum Medium without serum (Invitrogen) and added to the cell culture. The medium was changed after 6 h.

qRT-PCR

Total RNA was extracted from cells or tissues and complementary DNA was synthesized. Quality and quantity of the RNAs were assessed by A260/A280 nm optical density readings, using Biophotometer Plus (Eppendorf, Hamburg, Germany). RNA integrity was determined by running an aliquot of the RNA samples on a denaturing agarose gel stained with ethidium bromide. The total RNA then was diluted to 1 $\mu g \cdot \mu L^{-1}$ for further use. The transcript levels were detected via real-time reverse transcription PCR (qRT-PCR, ABI 7300) according to the manufacturer's instructions. Individual gene and microRNA expression was normalized to β-actin mRNA or small nuclear RNA (snRNA) U6 expression respectively. Primers used were listed in the Supporting Information Table S1.

Western blotting

Tissue homogenate or cell lysates were prepared. Proteins were separated by SDS-PAGE and transferred onto PVDF membranes (Biotrace, Randburg, South Africa). The membranes were blocked using skim milk and then incubated with diluted primary antibody overnight at 4°C with gentle shaking. After five washes, secondary HRP-conjugated antibody was incubated for 1 h at room temperature. After washing as before, positive signal was detected with fluorography using an enhanced chemiluminescence system (#7003; Cell Signaling Technology, Danvers, MA, USA). Antibodies used were listed in the Supporting Information Table S2. All Western blot results were scanned and semi-quantized by Image Pro-Plus 6.0 software (Media Cybernetics, Rockville, MD, USA). Background of the scanned image was clarified with the Image Pro-Plus image analysis system using brightness, contrast and gamma settings. The background of the image was further set as a fixed number using 'operation' tool. Then, the 'segmentation' tool was used to isolate the positive signal on the scanned image, and a new preview image was created. The newly created image was further converted to grey 8 bit image, and the boundaries of protein bands were defined by the AOI tool. The pixel number and density of protein bands were assessed, and each target protein density was normalized to the corresponding GAPDH density. The data were expressed as means ± SD by quantifying three independent Western blot results.

Sirius Red and H&E staining

Paraffin-embedded liver tissues in each group were stained with H&E and Sirius Red and were photographed at 100× and 40× magnification respectively. Briefly, paraffin-embedded liver tissues were sectioned at 5 µm; after deparaffinization and hydration, sections were stained with 0.1% (w/v) Sirius Red (Direct Red 80; Sigma-Aldrich) in a saturated aqueous solution of picric acid for 1 h. Then, the slides were rinsed twice, each for 15 min in 0.01 N HCl, to remove unbound dye. After dehydration, the slides were mounted.

Immunohistochemistry

Immunohistochemistry was performed on the paraffin-embedded liver sections. Sections were deparaffinized and hydrated as above, then slides were boiled in 1× citrate buffer for 10 min for epitope retrieval. The primary antibody was mounted on each section at 4°C overnight in a humid chamber. After washing three times in 1× Tris-HCl buffer, the secondary HRP-conjugated anti-primary IgG was incubated at room temperature for 1 h. After washing three times in 1× Tris-HCl buffer, the positive signal was detected by DAB substrate to achieve colorimetric end products. The slides were mounted and photographed with a Nikon TE-2000U camera (Nikon, Tokyo, Japan).

ELISA analysis

The ELISA against mouse TGF-β1 was performed following the manufacturer's instruction (88-8350-22; eBioscience, San Diego, CA, USA). Generally, the microtitre plate wells were coated with the liver tissue homogenate supernatant at appropriate dilution, or standard samples to make a standard curve, for 1 h at 37°C. The wells were washed with the washing buffer three times and the remaining liquid was drained on a stack of paper towels. The biotin-conjugated antibody was added to the wells for 1 h and washed as above, and the avidin-conjugated HRP enzyme was added for 30 min. Lastly, reacting substrate was added into every well and spectrophotometric analysis was conducted with microplate reader at 450 nm.

Luciferase assay

The AP-1 responsive element (7× TRE element, with the sequence 7× TGCTGAGTCA) or scrambled element was cloned into the mluI/BglII sites in the pGL3-promoter vector with a luciferase gene (E1761; Promega, San Luis Obispo, CA, USA). The constructs were transfected into HSC-T6 cells; the cells were treated with DIM/vehicle and further stimulated with TGF-β for 24 h. The plasmid encoding β-gal was co-transfected and used for normalization. The cells were harvested and lysed to measure luciferase activity.

Semi-quantitative analysis

For semi-quantitative analysis of collagen deposition, tissues stained with Sirius Red were photographed at 100× magnification; six randomly selected views in each group were chosen to be analysed with Image Pro-Plus 6.0 software.

Statistical analysis

Results are given as means ± SD. Data were analysed with one-way ANOVA. $P < 0.05$ was considered significant.

Materials

DIM was purchased from Ruima Chemical Co. (Nanjing, China; purity >99%). DIM is water insoluble, and an oil-dissolved DIM formulation was used, as in previous experiments (Riby *et al.*, 2006; Kim *et al.*, 2009). When this formulation is injected *in vivo*, the DIM-containing oil drops are mainly captured by the reticulo-endothelial system and hardly enter other tissues and cells. To solve this problem, DIM was formulated in 2-hydroxypropyl-β-cyclodextrin (Sigma-Aldrich, St. Louis, MO, USA) to enhance its water solubility according to our previous study (Dong *et al.*, 2010). Briefly, 20 mg DIM was dissolved in 1 mL of 2-hydroxypropyl-β-cyclodextrin solution (molar ratio 1:10). These stock solutions (20 mg·mL^{-1}) were serially diluted in sterile PBS to give final concentrations for *in vitro* or *in vivo* experiments on the day of use. This formulation of DIM can be injected into animals rather than being given orally, which can help to obtain more stable and credible experimental results when investigating its pharmacological mechanisms.

The antagonist oligonucleotide against miR-21 (antagomir-21) with the sequence 5′-CAACATCAGTCTGAT AAGC-3′ was verified. Antagomir-21 and scrambled (control) antagomirs with full phosphorothioate linkage were synthesized by SBS Genetech Co., Ltd (Shanghai, China).

Human recombinant TGF-β1 was purchased from PeproTech (Rocky Hill, NJ, USA).

Results

DIM inhibited HSC-T6 cell activation by modulating the TGF-β/Smad signalling cascade

To analyse the effects of DIM on cell viability, HSC-T6 cells were cultured with different concentrations of DIM or DMSO (solvent), and subjected to viability analysis. DIM at 20 and 40 μg·mL^{-1} affected cell viability but concentrations of 5 and 10 μg·mL^{-1} had no obvious cytotoxicity and were further tested (see Supporting Information Figure S1A). To determine the effects of DIM on the activation status of HSCs, the expression of α-SMA mRNA was used as a marker and was measured by qRT-PCR. DIM (5 μg·mL^{-1}) exerted no obvious effect on HSC-T6 activation, whereas a higher concentration (10 μg·mL^{-1}) significantly suppressed HSC-T6 activation (Figure 1A). Thus, the 10 μg·mL^{-1} concentration was chosen for further experiments. Activated HSCs are characterized by a dramatically increased synthesis of collagen type I (COL1A1), which predominates over normal collagen type IV (Hernandez-Gea and Friedman, 2011). Therefore, the expression of COL1A1 mRNA was measured in HSC-T6 cells. DIM effectively blocked the up-regulation of COL1A1 expression induced by the profibrogenic cytokine TGF-β (Figure 1B). We also measured the expression of α-SMA and COL1A1 proteins in HSC-T6 cells and found them to be reduced by DIM treatment (Figure 1C,D).

The TGF-β/Smad signalling cascade is the central pathway that leads to HSC activation; Smad2/3 is the main effector in this pathway, whereas the Smad7 exerts antagonistic effects in this signalling cascade. Thus, the expression of Smad proteins were measured in HSC-T6 cells after DIM treatment. TGF-β markedly increased the phosphorylation of Smad2/3 (p-Smad2/3), which was attenuated by DIM (Figure 1E). Moreover, DIM maintained the high levels of Smad7 in HSC-T6 cells (Figure 1F). Interestingly, the total Smad2/3 expression in HSC-T6 cells was down-regulated after DIM treatment (Figure 1E). Further, DIM treatment did not affect the expression of PCNA mRNA in HSCs, implying that DIM had no influence on the non-canonical TGF-β pathway (Supporting Information Figure S1B). Taken together, our data showed that DIM could suppress HSC activation by inhibiting the TGF-β/Smad signalling pathway.

DIM inhibited the TGF-β/Smad signalling cascade through modulating miR-21 expression

miR-21 is one of the most important miRNAs during fibrosis in different tissues, which could degrade the anti-fibrotic protein Smad7 (Liu *et al.*, 2010; Marquez *et al.*, 2010). To test whether DIM could modulate miR-21 expression, HSC-T6 cells were cultured with DIM, and the miR-21 expression in HSC-T6 cells was determined by qRT-PCR. DIM treatment significantly down-regulated miR-21 expression in HSC-T6 cells (Figure 2A). Furthermore, transfection of HSC-T6 cells with antagomir-21 reduced miR-21 levels in HSC-T6 cells (Supporting Information Figure S1C). Along with the down-regulated miR-21 levels, HSC-T6 cells exhibited a lower level of α-SMA expression and COL1A1 deposition (Figure 2B,C).

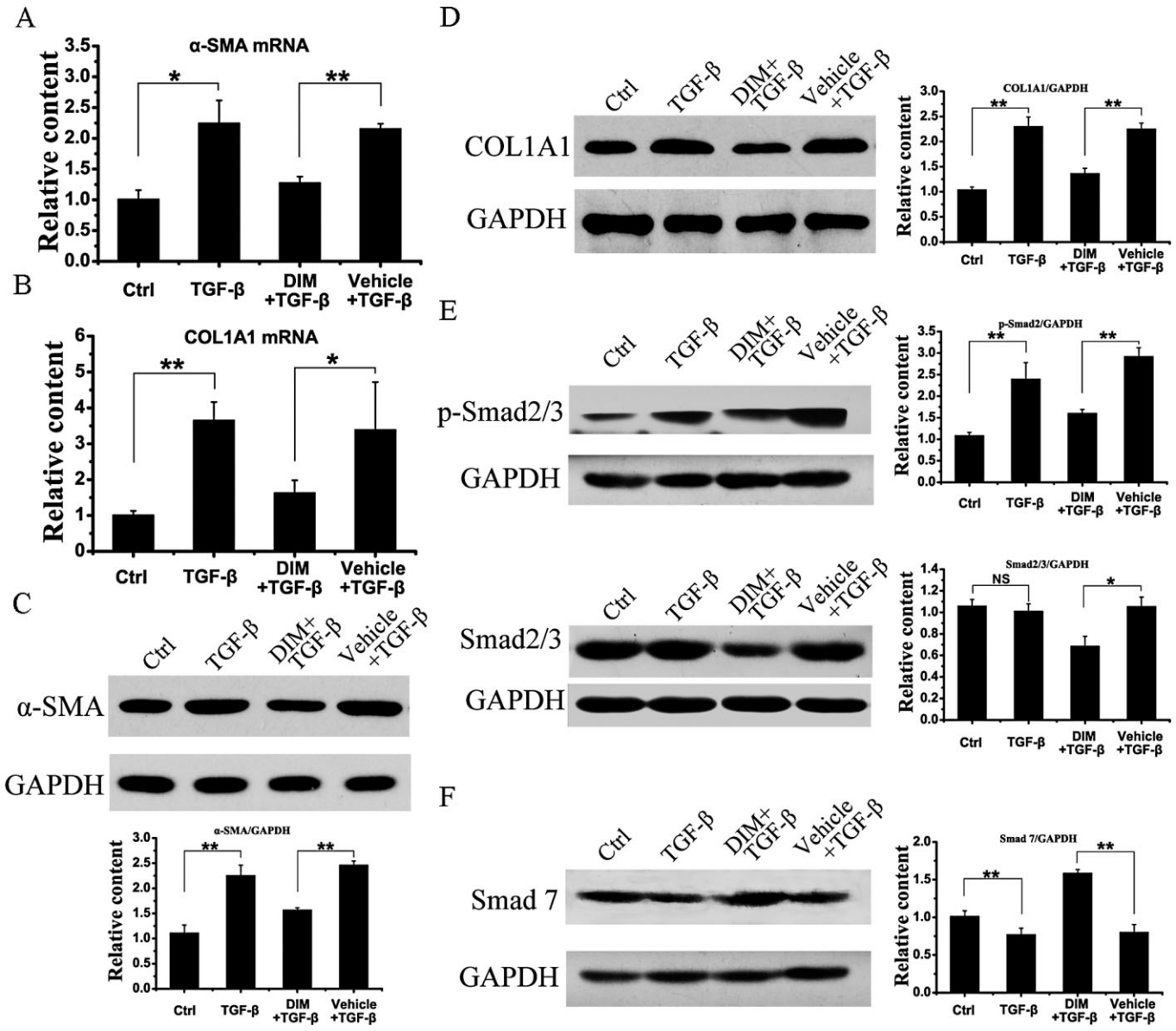

Figure 1

DIM suppressed HSC activation by inhibiting the TGF-β signalling cascade. HSC-T6 cells were co-cultured with 10 mg·mL^{-1} DIM for 24 h and then stimulated with 5 ng·mL^{-1} TGF-β1 for 24 h. (A) α-SMA mRNA levels in HSC-T6 cells were determined by qRT-PCR. (B) COL1A1 mRNA levels in HSC-T6 cells were determined by qRT-PCR. (C) α-SMA protein levels in HSC-T6 cells were measured by Western blotting. (D) COL1A1 protein levels in HSC-T6 cells were measured by Western blotting. (E) p-Smad2/3 and Smad2/3 protein levels in HSC-T6 cells were measured by Western blotting. (F) Smad7 protein levels in HSC-T6 cells were measured by Western blotting. Western blot was repeated twice with similar trends. Western blot results were semi-quantitatively analysed by Image Pro-Plus 6.0 software. Data are expressed as means ± SD of three independent experiments and each experiment contained at least three samples; *P < 0.05, **P < 0.01, significantly different as shown.

Further analysis of the TGF-β signalling cascade indicated that decreasing the miR-21 content in HSC-T6 cells inhibited phosphorylation of Smad2/3 induced by TGF-β stimulation (Figure 2D), whereas the levels of the inhibitory Smad7 were maintained after down-regulation of miR-21 by antagomir-21 (Figure 2E). Compared with antagomir-21 transfection, DIM treatment achieved a similar, but slightly greater, inhibition of HSC-T6 activation and the TGF-β signalling pathway.

DIM decreased miR-21 expression by inhibiting AP-1 activity

The gene for miR-21 includes binding sequences for several transcription factors, including those for the AP-1 family, among which the heterodimer formed by c-Jun and Fra-1, in particular, has been shown to drive the expression of miR-21. (Fujita *et al.*, 2008; Talotta *et al.*, 2009; Frezzetti *et al.*, 2011). To show that miR-21 could modulate the AP-1 activity, the

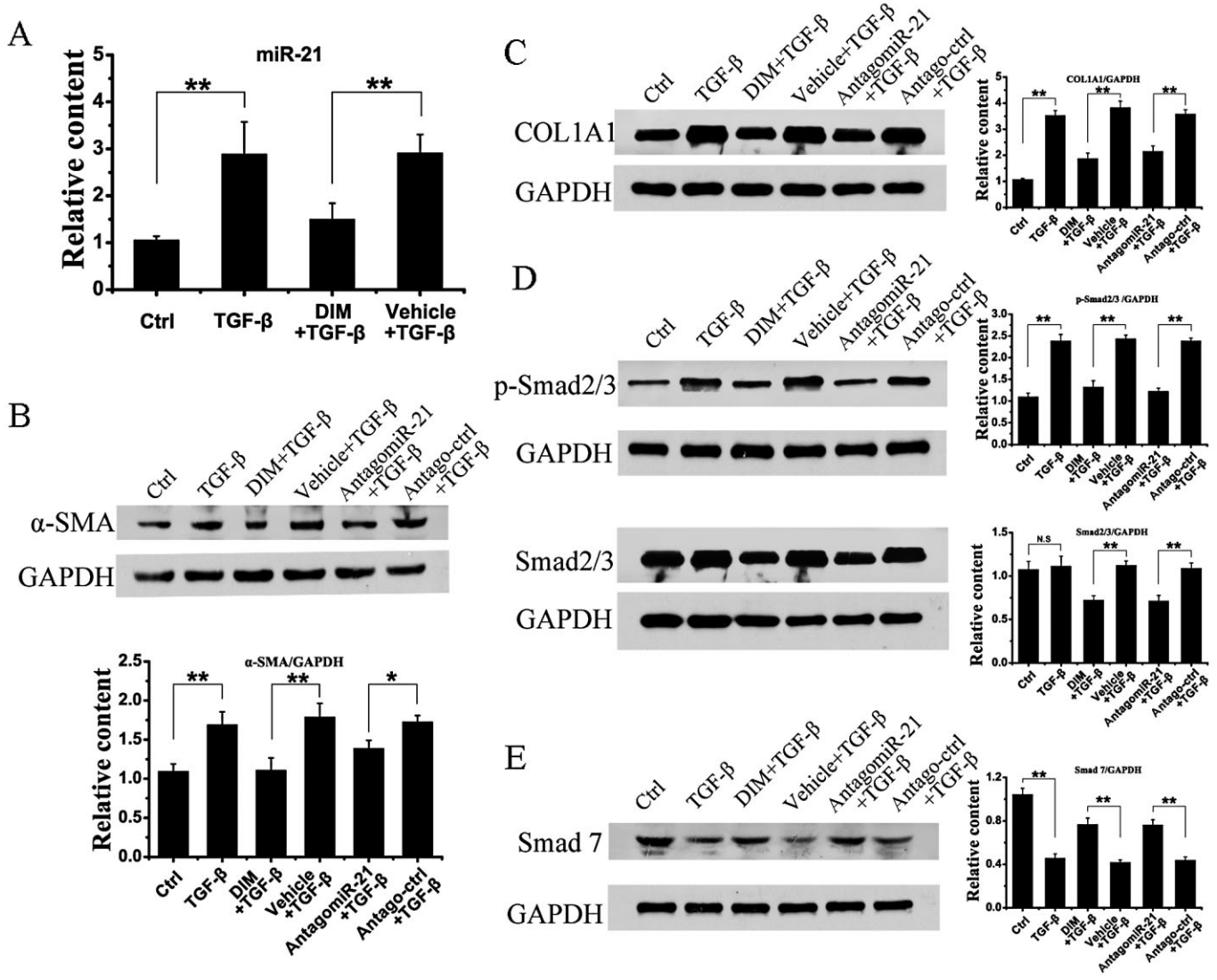

Figure 2

DIM inhibited TGF-β signalling pathway by down-regulating the miR-21 expression. HSC-T6 cells were co-cultured with 10 mg·mL^{-1} DIM or transfected with 50 nM antagomir-21/antago-ctrl, and cells were further stimulated with 5 ng·mL^{-1} TGF-β1 for 24 h. (A) miR-21 levels in HSC-T6 cells after DIM treatment were determined by qRT-PCR. (B) α-SMA and (C) COL1A1 protein levels in HSC-T6 cells were measured by Western blotting. (D) p-Smad2/3 and Smad2/3 protein levels in HSC-T6 cells were measured by Western blotting. (E) Smad7 protein levels in HSC-T6 cells were measured by Western blotting. A representative example of three independent Western blot results is presented. Western blot results were semi-quantitatively analysed by Image Pro-Plus 6.0 software. Data are expressed as means ± SD of three independent experiments and each experiment contained at least three samples; *$P < 0.05$, **$P < 0.01$, significantly different as shown.

AP-1 response element (7× TRE) was cloned into a plasmid containing the luciferase reporter gene (Lee *et al.*, 1987). Stimulation with TGF-β increased AP-1 activity and this increase was blocked by DIM treatment (Figure 3A). Furthermore, expression of c-Jun and Fra-1 in HSC-T6 cells was decreased by DIM (Figure 3B,C).

DIM inhibited the activation of primary HSCs

When plated on uncoated plastic vessels, freshly isolated primary HSCs undergo a self-activation process that closely mimics the *in vivo* activation process during the pathogenesis of hepatic fibrosis (Friedman, 1993). Rat primary HSCs were isolated, and identified by α-SMA immunofluorescence staining, as indicated in the Supporting Information Figure S1D. Primary HSCs were cultured with DIM/DMSO or transfected with antagomir-21/antago-ctrl during a 15 day culture on plastic. Expression of miR-21 was markedly up-regulated in primary HSCs during this culture. Co-culture with DIM or transfection with antagomir-21 down-regulated miR-21 expression in these primary HSCs (Figure 4A). DIM also decreased the levels of mRNA and protein for α-SMA and COL1A1 (Figure 4B,C,D). Moreover, following DIM treatment, levels of phosphorylated Smad2/3 in the primary HSCs

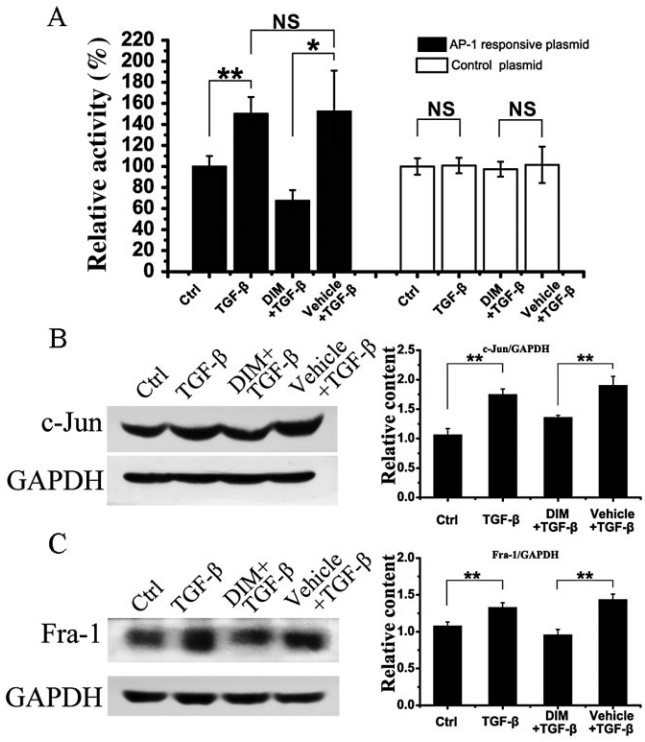

Figure 3

DIM down-regulated miR-21 expression by inhibiting AP-1 activity. HSC-T6 cells were treated with 10 mg·mL^{-1} DIM for 24 h and then stimulated with 5 ng·mL^{-1} TGF-β1 as indicated. (A) AP-1 responsive plasmid luciferase activity was measured in HSC-T6 cells after DIM treatment. (B) c-Jun protein levels in HSC-T6 cells were measured by Western blotting. (C) Fra-1 protein levels in HSC-T6 cells were measured by Western blotting. A representative example of three independent Western blot results is presented. Western blot results were semi-quantitatively analysed by Image Pro-Plus 6.0 software. Data are expressed as means ± SD of three independent experiments and each experiment contained at least three samples; *P < 0.05, **P < 0.01, significantly different as shown.

were decreased (Figure 4E), whereas those of Smad7 remained high, at the end of the 15 days of culture (Figure 4F). Taken together, DIM treatment suppressed activation in primary HSC in culture.

DIM protected against TAA-induced hepatic fibrosis

To determine the effect of DIM on pathogenesis and progression of liver fibrosis *in vivo*, the effects of three doses of DIM were studied on the induction of hepatic fibrosis in mice by TAA, given over 8 weeks. To determine collagen deposition in the liver, liver samples were analysed for hydroxyproline which is one of the main components of collagen proteins. Compared with mice that received vehicle treatment, DIM at the highest dose tested (50 mg·kg^{-1}) significantly reduced the hydroxyproline content of liver, whereas 2 and 10 mg·kg^{-1} DIM had no obvious effects (Figure 5A). Furthermore, sections of liver were stained with Sirius Red to indicate the total collagen deposition, as shown in Figure 5B. DIM (50 mg·kg^{-1}) ameliorated liver fibrosis and reduced the collagen deposition (Figure 5C and Supporting Information Figure S1E). This DIM treatment also decreased the mRNA and protein expression of α-SMA and COL1A1 in liver from mice treated with TAA. (Figure 5D,E,F).

DIM in vivo down-regulated miR-21 expression and attenuated Smad2/3 phosphorylation in the liver

Total RNA was extracted from livers of different groups of mice and subjected to qRT-PCR analysis. Expression of miR-21 was markedly up-regulated by treatment of mice *in vivo* with TAA. Given that miR-21 is one of the most abundant microRNAs (Lagos-Quintana *et al.*, 2003), the up-regulation of miR-21 represented a very large absolute increase and this increase was down-regulated by treatment with DIM (50 mg·kg^{-1}) (Figure 6A). We also assessed levels of phosphorylated-Smad2/3 in liver sections by immunohistochemistry. As indicated in Figure 6B, after 50 mg·kg^{-1} DIM treatment, phosphorylated Smad2/3 was much decreased in the liver, suggesting decreased activation of the TGF-β signalling cascade. DIM (50 mg·kg^{-1}) also inhibited the higher levels of TGF-β1 in liver homogenates induced by TAA (Figure 6C), indicating that DIM could also ameliorate hepatic fibrosis by directly down-regulating TGF-β1. However, levels of aspartate (AST) or alanine aminotranferases (ALT) were not decreased by DIM treatment (Figure 6D), indicating that the therapeutic effects were achieved by directly affecting fibrogenesis and not by preventing the necrosis, induced by TAA, in hepatocytes.

Discussion

Progress has been achieved by elucidating the central TGF-β/Smad2/3 signal pathway underlying HSC activation and blocking the canonical TGF-β/Smad2/3 signal cascade represents the primary strategy for the treatment of liver fibrosis (Qi *et al.*, 1999). Strategies such as soluble antibodies (George *et al.*, 1999) or virus-mediated gene silencing of components in this signalling pathway have achieved successful therapeutic effects in laboratory studies (Nakamura *et al.*, 2000; Dooley *et al.*, 2003; Jiang *et al.*, 2004). However, their effectiveness, stability and safety in patients are still debated, thus limiting their clinical application.

miRNAs play essential roles in numerous cellular and developmental processes. Aberrant expression of miRNAs is closely associated with initiation and progression of different pathophysiological processes (Mendell and Olson, 2012). miR-21 is up-regulated in different types of cancer, and recent studies suggest that high levels of miR-21 may not only characterize cancer cells but also represent a common feature of pathological responses to excessive cellular stress (Krichevsky and Gabriely, 2009). Other studies have indicated that miR-21 is up-regulated during fibrogenesis in the heart, kidney and lung (Thum *et al.*, 2008; Liu *et al.*, 2010; Zhong *et al.*, 2011). In addition, miR-21 was significantly up-regulated in liver fibrosis of different aetiologies (Jiang *et al.*, 2008; Marquez *et al.*, 2010; Wang *et al.*, 2012), further indicating miR-21 as a common effector in fibrotic disease. This implies that miR-21 may serve as an attractive therapeutic

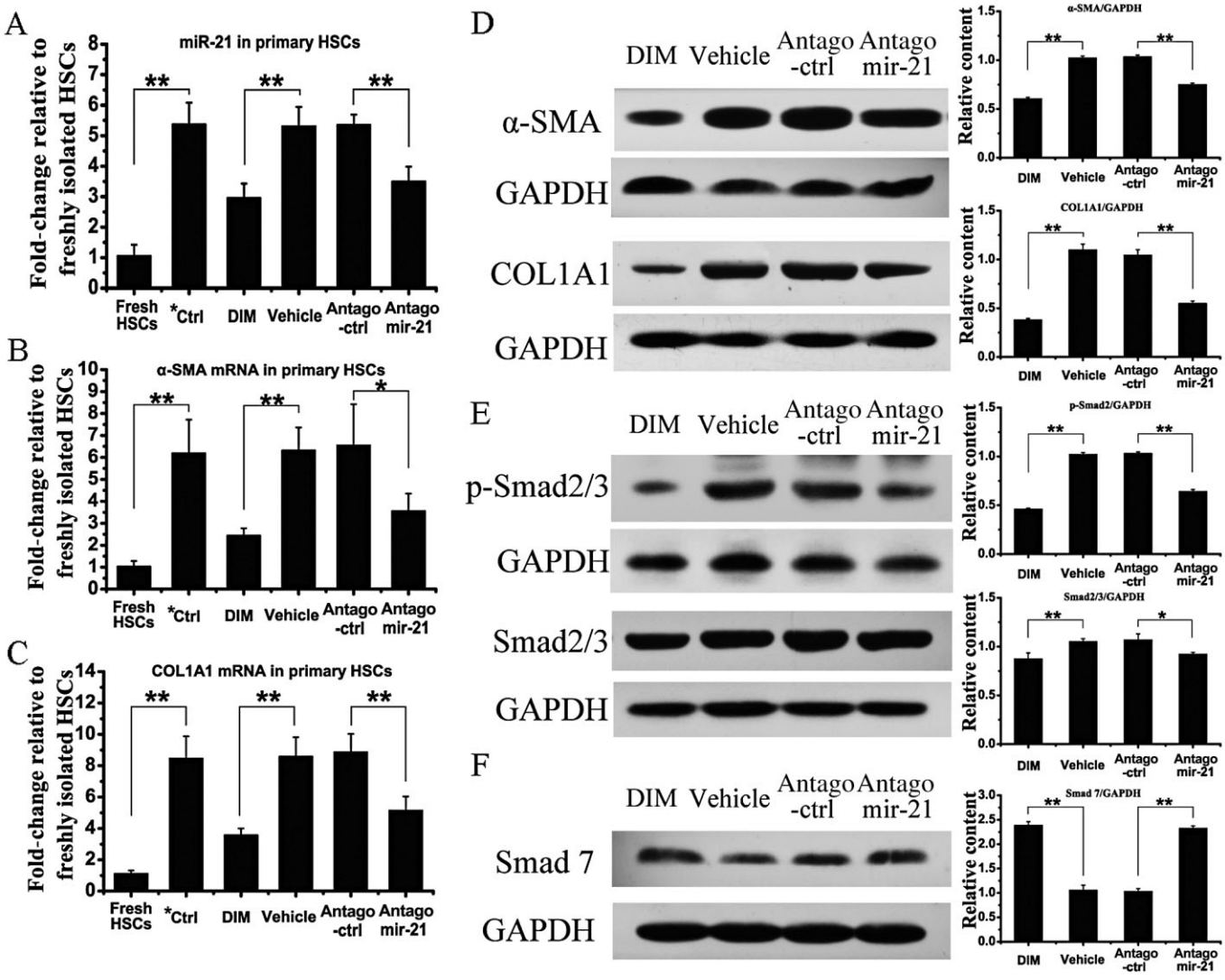

Figure 4

DIM inhibited self-activation of primary HSCs. Rat primary HSCs were isolated and cultured on uncoated plastic vessels for 15 days. The HSCs were co-cultured with 10 mg·mL^{-1} DIM for the same time or transfected with 50 nM antagomir-21/antago-ctrl respectively. (A) miR-21 levels in primary HSCs after treatment were measured by qRT-PCR. (B) α-SMA mRNA levels in primary HSCs were determined by qRT-PCR. (C) COL1A1 mRNA levels in primary HSCs were determined by qRT-PCR. (D) α-SMA and COL1A1 protein levels in primary HSCs were measured by Western blotting. (E) p-Smad2/3 and Smad2/3 protein levels in primary HSCs were measured by Western blotting. (F) Smad7 protein levels in primary HSCs were measured by Western blotting. A representative example of three independent Western blot results is presented. Western blot results were semi-quantitatively analysed by Image Pro-Plus 6.0 software. *Ctrl indicated the isolated primary HSCs cultured on plastic for 15 days without any treatment. Data are expressed as means ± SD of three independent experiments and each experiment contained at least three samples; *$P < 0.05$, **$P < 0.01$, significantly different as shown.

target against liver fibrosis under different pathological conditions. Moreover, inhibiting miR-21 expression in the lung successfully ameliorated pulmonary fibrosis and further analysis suggests that miR-21 promotes fibrosis by targeting the anti-fibrotic protein Smad7 (Liu *et al.*, 2010). Smad7, as an intrinsic inhibitor of the TGF-β/Smad2/3 pathway, competes with R-Smads for type I TGF receptors (TβRI) and intervenes in TGF-β/Smad2/3 signal transduction. Previous studies have indicated that adenovirus-mediated Smad7 overexpression in rat livers inhibited collagen deposition and α-SMA expression in HSCs (Dooley *et al.*, 2003).

DIM is a natural product from the *Brassica* genus and has been taken by people as a health product for years, proving its safety for humans. Most of the studies with DIM have focused on its anti-cancer activity, and clinical trials are now being carried out on DIM for the treatment of cancer. Our present study demonstrates that DIM down-regulated miR-21 expression in both HSC-T6 cells and primary HSCs, and further *in vivo* studies in mice revealed that DIM down-regulated miR-21 expression during induction of fibrosis. As a consequence, the anti-fibrotic Smad7 protein was maintained at high levels during liver fibrogenesis and exerted sustained

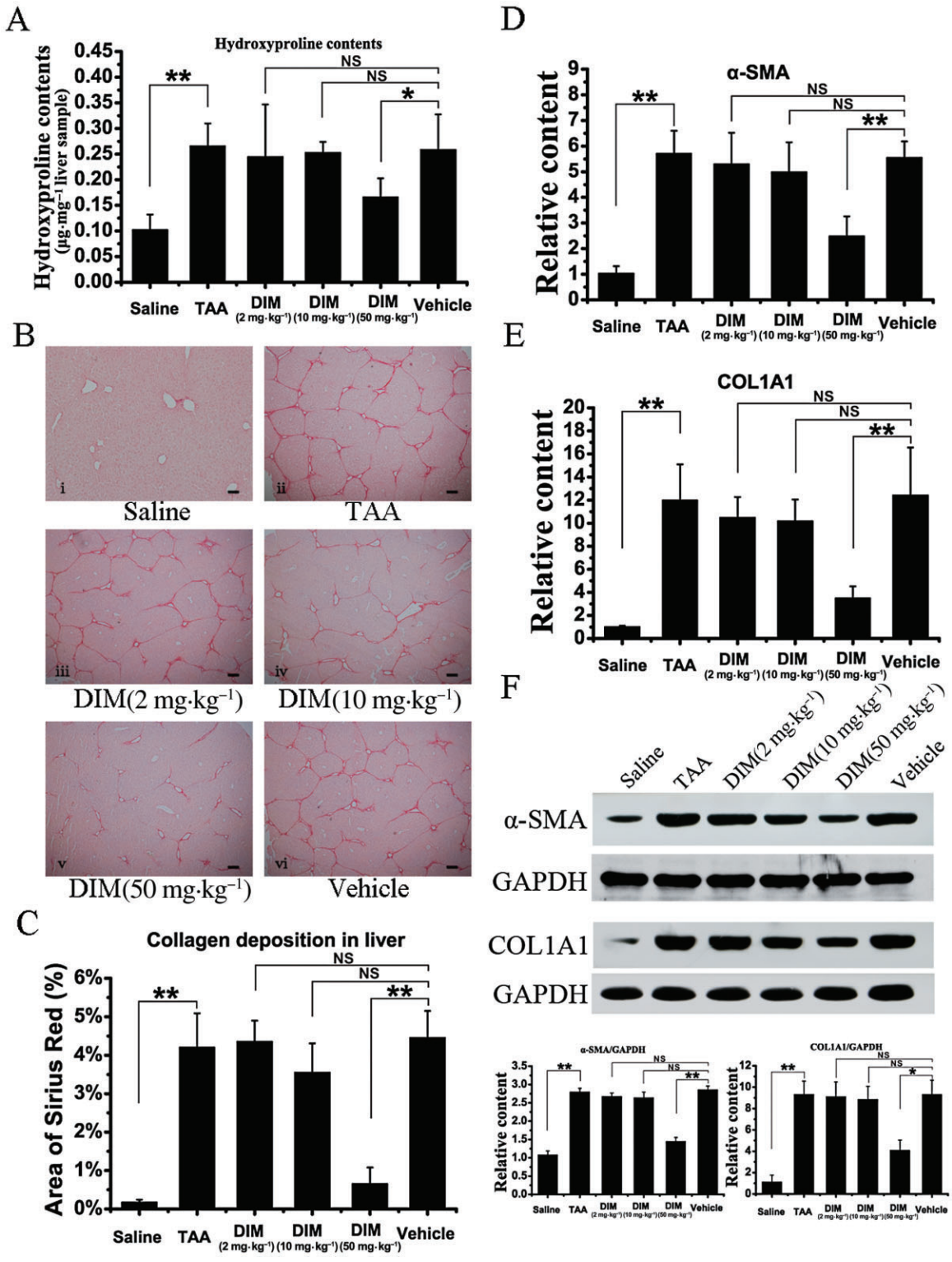

Figure 5

DIM protected against TAA-induced hepatic fibrosis in mice. During the 8 weeks exposure to TAA, DIM was also administered. (A) Hydroxyproline content of liver samples after DIM treatment. (B) Representative image of Sirius Red staining of liver sections in indicated groups. (C) Semi-quantitative analysis of collagen deposition of Sirius Red staining. (D) α-SMA mRNA levels in total liver in indicated groups were determined by qRT-PCR. (E) COL1A1 mRNA levels in total liver in indicated groups were determined by qRT-PCR. (F) α-SMA and COL1A1 protein levels in liver samples of different groups were measured by Western blotting. A representative example of three independent Western blot results is presented. Western blot results were semi-quantitatively analysed by Image Pro-Plus 6.0 software. Data are expressed as means ± SD of three independent experiments ($n = 6$ mice); $^*P < 0.05$, $^{**}P < 0.01$, significantly different as shown.

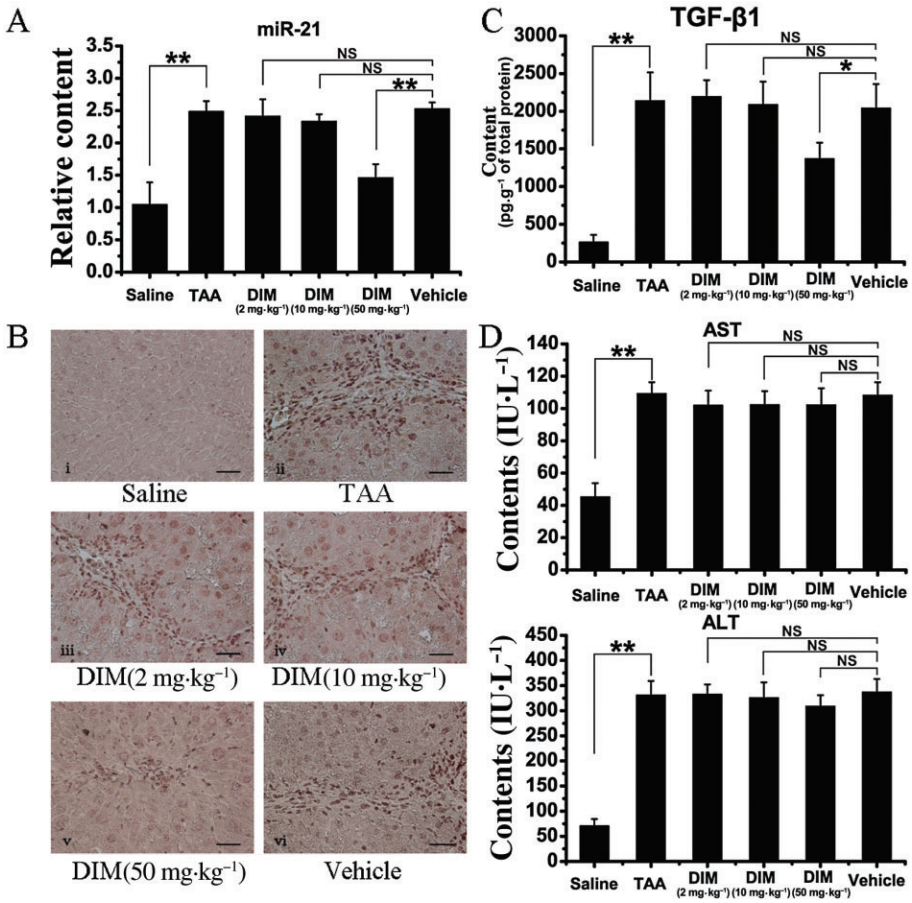

Figure 6

DIM down-regulated miR-21 expression and the TGF-β signalling cascade in fibrotic liver, induced by TAA. During the 8 weeks exposure of mice to TAA, DIM was also administered. (A) miR-21 levels in total liver in indicated groups were determined by qRT-PCR. (B) Representative p-Smad2/3 IHC images of liver sections in different groups. (C) TGF-β1 concentrations in liver tissue homogenate were determined by ELISA. (D) Serum AST and ALT levels were determined. A representative example of three independent results is presented. Data are expressed as means ± SD of three independent experiments (n = 6 mice); *P < 0.05, **P < 0.01, significantly different as shown.

antagonistic effects on the central TGF-β signalling cascade, resulting in a much lower profibrogenic gene expression. Furthermore, Smad2/3, as the main signalling mediator, plays a pivotal role in the TGF-β signalling pathway. Thus, Smad2/3 mediated the expression of COL1A1 in activated HSCs and targeted deletion of Smad2/3 prevented or halted the progression of hepatic fibrosis in animals (Schnabl *et al.*, 2001). Interestingly, in our present study, DIM could down-regulate Smad2/3 expression in HSC-T6 cells. This could reduce the expression of profibrogenic genes and exert a direct suppression on HSC activation. Taken together, DIM could modulate the TGF-β signalling pathway by protecting against the degradation mediated by miR-21 of the antagonistic Smad7 and by down-regulating the main signalling transducers, Smad2/3. DIM inhibited MCF-7 cell proliferation and this inhibitory effect was achieved, at least in part, by increasing miR-21 expression (Jin, 2011). This is a surprising finding as miR-21 is commonly considered as an oncomiR according to Krichevsky and Gabriely (2009). This finding may imply that miR-21 expression may be differently modulated by DIM depending on the cell type and under different cellular contexts.

Several transcription factors including those of the AP-1 family have been shown to promote miR-21 expression (Fujita *et al.*, 2008; Talotta *et al.*, 2009; Frezzetti *et al.*, 2011). The signalling kinase, JNK, whose activity is mainly mediated by AP-1 is found in high levels in myofibroblasts during hepatic fibrosis (Kluwe *et al.*, 2010). This highlights the prominent role of AP-1 in HSC activation and disease progression. Our present study further demonstrated that DIM could inhibit AP-1 activity and thus down-regulate miR-21 expression in HSCs. AP-1 can also interact with structurally unrelated DNA-binding proteins, including the Smad family proteins (Shaulian and Karin, 2002). Intrinsically, without auxiliary factors, Smad proteins bind to DNA with low affinity and specificity. Among their cooperating partners, AP-1 can bind to Smad2/3 and facilitate the binding to the cis-acting elements, thus promoting the translation of profibrogenic genes in response to TGF-β (Shaulian and Karin, 2002; Schmierer and Hill, 2007). Therefore, it is possible that AP-1 could promote profibrogenic activities in HSCs by this synergic effect. Furthermore, during activation, HSCs undergo two stages: initiation and perpetuation (Friedman, 2008). After the initiation phase, HSCs maintain a sustained activa-

tion state. This could be partially attributed to the auto-induction of TGF-β, as TGF-β can activate its own expression and secretion in an AP-1-dependent way in HSCs (Kim *et al.*, 1990). Therefore, in addition to the down-regulation of miR-21 expression, DIM could interrupt the TGF-β autocrine pathway by inhibiting AP-1 activity and thus suppress HSC activation.

In conclusion, our present study demonstrated the protective role of DIM against experimental hepatic fibrosis induced by TAA. Further analysis of the underlying mechanisms suggests that DIM could successfully suppress HSC activation by down-regulating miR-21 expression, through inhibiting AP-1 activity. The current therapy for end-stage cirrhotic patients is liver transplantation, which is limited by the shortage of appropriate donor livers. In patients with cirrhosis, there is a high risk of progressing to HCC, a condition with high mortality. Thus, slowing down the progression of fibrosis could reduce the risk of cancer development and ameliorate the complications associated with fibrosis. In this regard, DIM may have potential as a novel anti-fibrotic treatment for patients with different chronic liver diseases.

Acknowledgements

This work was supported by the National Science Fund for Distinguished Young Scholars (81025019), National Natural Science Foundation of China (31071232, 31170751, 51173076, 91129712 and 81102489), Key Project of Chinese Ministry of Education (108059), the PhD Programs Foundation of Ministry of Education of China (20100091120020) and Jiangsu Provincial Natural Science Foundation of China (BK 2009237).

Conflict of interest

Nothing to report.

References

Beaven SW, Wroblewski K, Wang J, Hong C, Bensinger S, Tsukamoto H *et al.* (2011). Liver X receptor signaling is a determinant of stellate cell activation and susceptibility to fibrotic liver disease. Gastroenterology 140: 1052–1062.

Chung AC, Dong Y, Yang W, Zhong X, Li R, Lan HY (2013). Smad7 suppresses renal fibrosis via altering expression of TGF-β/Smad3-regulated microRNAs. Mol Ther 21: 388–398.

Dong L, Xia S, Gao F, Zhang D, Chen J, Zhang J (2010). 3,3′-Diindolylmethane attenuates experimental arthritis and osteoclastogenesis. Biochem Pharmacol 79: 715–721.

Dooley S, Hamzavi J, Breitkopf K, Wiercinska E, Said HM, Lorenzen J *et al.* (2003). Smad7 prevents activation of hepatic stellate cells and liver fibrosis in rats. Gastroenterology 125: 178–191.

Frezzetti D, De Menna M, Zoppoli P, Guerra C, Ferraro A, Bello AM *et al.* (2011). Upregulation of miR-21 by Ras *in vivo* and its role in tumor growth. Oncogene 30: 275–286.

Friedman SL (1993). Seminars in medicine of the Beth Israel Hospital, Boston. The cellular basis of hepatic fibrosis. Mechanisms and treatment strategies. N Engl J Med 328: 1828–1835.

Friedman SL (2008). Mechanisms of hepatic fibrogenesis. Gastroenterology 134: 1655–1669.

Fujita S, Ito T, Mizutani T, Minoguchi S, Yamamichi N, Sakurai K *et al.* (2008). miR-21 gene expression triggered by AP-1 is sustained through a double-negative feedback mechanism. J Mol Biol 378: 492–504.

George J, Roulot D, Koteliansky VE, Bissell DM (1999). *In vivo* inhibition of rat stellate cell activation by soluble transforming growth factor beta type II receptor: a potential new therapy for hepatic fibrosis. Proc Natl Acad Sci U S A 96: 12719–12724.

Hernandez-Gea V, Friedman SL (2011). Pathogenesis of liver fibrosis. Annu Rev Pathol 6: 425–456.

Jiang J, Gusev Y, Aderca I, Mettler TA, Nagorney DM, Brackett DJ *et al.* (2008). Association of microRNA expression in hepatocellular carcinomas with hepatitis infection, cirrhosis, and patient survival. Clin Cancer Res 14: 419–427.

Jiang W, Yang CQ, Liu WB, Wang YQ, He BM, Wang JY (2004). Blockage of transforming growth factor beta receptors prevents progression of pig serum-induced rat liver fibrosis. World J Gastroenterol 10: 1634–1638.

Jin Y (2011). 3,3′-Diindolylmethane inhibits breast cancer cell growth via miR-21-mediated Cdc25A degradation. Mol Cell Biochem 358: 345–354.

Kilkenny C, Browne W, Cuthill IC, Emerson M, Altman DG (2010). Animal research: reporting *in vivo* experiments: the ARRIVE guidelines. Br J Pharmacol 160: 1577–1579.

Kim SJ, Angel P, Lafyatis R, Hattori K, Kim KY, Sporn MB *et al.* (1990). Autoinduction of transforming growth factor beta 1 is mediated by the AP-1 complex. Mol Cell Biol 10: 1492–1497.

Kim YH, Kwon HS, Kim DH, Shin EK, Kang YH, Park JH *et al.* (2009). 3,3′-Diindolylmethane attenuates colonic inflammation and tumorigenesis in mice. Inflamm Bowel Dis 15: 1164–1173.

Kluwe J, Pradere JP, Gwak GY, Mencin A, De Minicis S, Osterreicher CH *et al.* (2010). Modulation of hepatic fibrosis by c-Jun-N-terminal kinase inhibition. Gastroenterology 138: 347–359.

Krichevsky AM, Gabriely G (2009). miR-21: a small multi-faceted RNA. J Cell Mol Med 13: 39–53.

Lagos-Quintana M, Rauhut R, Meyer J, Borkhardt A, Tuschl T (2003). New microRNAs from mouse and human. RNA 9: 175–179.

Lee W, Mitchell P, Tjian R (1987). Purified transcription factor AP-1 interacts with TPA-inducible enhancer elements. Cell 49: 741–752.

Liu G, Friggeri A, Yang Y, Milosevic J, Ding Q, Thannickal VJ *et al.* (2010). miR-21 mediates fibrogenic activation of pulmonary fibroblasts and lung fibrosis. J Exp Med 207: 1589–1597.

Liu Y, Wang Z, Kwong SQ, Lui EL, Friedman SL, Li FR *et al.* (2011). Inhibition of PDGF, TGF-beta, and Abl signaling and reduction of liver fibrosis by the small molecule Bcr-Abl tyrosine kinase antagonist Nilotinib. J Hepatol 55: 612–625.

McGrath JC, Drummond GB, McLachlan EM, Kilkenny C, Wainwright CL (2010). Guidelines for reporting experiments involving animals: the ARRIVE guidelines. Br J Pharmacol 160: 1573–1576.

McGuire KP, Ngoubilly N, Neavyn M, Lanza-Jacoby S (2006). 3,3′-diindolylmethane and paclitaxel act synergistically to promote apoptosis in HER2/Neu human breast cancer cells. J Surg Res 132: 208–213.

Marquez RT, Bandyopadhyay S, Wendlandt EB, Keck K, Hoffer BA, Icardi MS *et al*. (2010). Correlation between microRNA expression levels and clinical parameters associated with chronic hepatitis C viral infection in humans. Lab Invest 90: 1727–1736.

Melkamu T, Zhang X, Tan J, Zeng Y, Kassie F (2010). Alteration of microRNA expression in vinyl carbamate-induced mouse lung tumors and modulation by the chemopreventive agent indole-3-carbinol. Carcinogenesis 31: 252–258.

Mendell JT, Olson EN (2012). MicroRNAs in stress signaling and human disease. Cell 148: 1172–1187.

Nakamura T, Sakata R, Ueno T, Sata M, Ueno H (2000). Inhibition of transforming growth factor beta prevents progression of liver fibrosis and enhances hepatocyte regeneration in dimethylnitrosamine-treated rats. Hepatology 32: 247–255.

Okino ST, Pookot D, Basak S, Dahiya R (2009). Toxic and chemopreventive ligands preferentially activate distinct aryl hydrocarbon receptor pathways: implications for cancer prevention. Cancer Prev Res (Phila) 2: 251–256.

Qi Z, Atsuchi N, Ooshima A, Takeshita A, Ueno H (1999). Blockade of type beta transforming growth factor signaling prevents liver fibrosis and dysfunction in the rat. Proc Natl Acad Sci U S A 96: 2345–2349.

Rahman KM, Banerjee S, Ali S, Ahmad A, Wang Z, Kong D *et al*. (2009). 3,3′-Diindolylmethane enhances taxotere-induced apoptosis in hormone-refractory prostate cancer cells through survivin down-regulation. Cancer Res 69: 4468–4475.

Riby JE, Xue L, Chatterji U, Bjeldanes EL, Firestone GL, Bjeldanes LF (2006). Activation and potentiation of interferon-gamma signaling by 3,3′-diindolylmethane in MCF-7 breast cancer cells. Mol Pharmacol 69: 430–439.

Saxena NK, Ikeda K, Rockey DC, Friedman SL, Anania FA (2002). Leptin in hepatic fibrosis: evidence for increased collagen production in stellate cells and lean littermates of ob/ob mice. Hepatology 35: 762–771.

Schmierer B, Hill CS (2007). TGFbeta-SMAD signal transduction: molecular specificity and functional flexibility. Nat Rev Mol Cell Biol 8: 970–982.

Schnabl B, Kweon YO, Frederick JP, Wang XF, Rippe RA, Brenner DA (2001). The role of Smad3 in mediating mouse hepatic stellate cell activation. Hepatology 34: 89–100.

Shaulian E, Karin M (2002). AP-1 as a regulator of cell life and death. Nat Cell Biol 4: E131–E136.

Talotta F, Cimmino A, Matarazzo MR, Casalino L, De Vita G, D'Esposito M *et al*. (2009). An autoregulatory loop mediated by miR-21 and PDCD4 controls the AP-1 activity in RAS transformation. Oncogene 28: 73–84.

Thum T, Gross C, Fiedler J, Fischer T, Kissler S, Bussen M *et al*. (2008). MicroRNA-21 contributes to myocardial disease by stimulating MAP kinase signalling in fibroblasts. Nature 456: 980–984.

Vogel S, Piantedosi R, Frank J, Lalazar A, Rockey DC, Friedman SL *et al*. (2000). An immortalized rat liver stellate cell line (HSC-T6): a new cell model for the study of retinoid metabolism *in vitro*. J Lipid Res 41: 882–893.

Wang XW, Heegaard NH, Orum H (2012). MicroRNAs in liver disease. Gastroenterology 142: 1431–1443.

Weiskirchen R, Gressner AM (2005). Isolation and culture of hepatic stellate cells. Methods Mol Med 117: 99–113.

Zhang C, Ding Z, Suhaimi NA, Kng YL, Zhang Y, Zhuo L (2009). A class of imidazolium salts is anti-oxidative and anti-fibrotic in hepatic stellate cells. Free Radic Res 43: 899–912.

Zhong X, Chung AC, Chen HY, Meng XM, Lan HY (2011). Smad3-mediated upregulation of miR-21 promotes renal fibrosis. J Am Soc Nephrol 22: 1668–1681.

Supporting information

Additional Supporting Information may be found in the online version of this article at the publisher's web-site:

Figure S1 (A) DIM cytotoxicity was measured by Cell Counting Kit-8 analysis. (B) Levels of PCNA mRNA in HSCs after DIM treatment. (C) miR-21 content in HSC-T6 cells after transfection with antagomir-21/antago-ctrl. (D) The isolated primary HSCs were identified by α-SMA staining. (E) A representative example of H&E staining of liver sections after DIM treatment. Data are expressed as the means ± SD of three independent experiments and each contained at least 3 samples, $*P < 0.05$, $**P < 0.01$.
Table S1 PCR primers used in this study.
Table S2 Primary and secondary antibodies used in Western blotting.